Finite-Time Sliding Mode Control of Vehicle Formation with Specified Performance

Dongyang Guo, Zhao Zhang, Hongyan Zhou, and Xue-Bo Chen

***Abstract*—The current urban intelligent transportation is in a rapid development stage, and coherence control of vehicle formations has important implications in urban intelligent transportation research. This article focuses on the problem of urban intelligent transportation planning, and proposes a new control method for vehicle formation regulation tracking performance control with bounded disturbances and model uncertainty, combining the multiple advantages of sliding mode control and finite time control and utilizing the universal approximation of neural network. This method can ensure that the vehicle formation can achieve the specified tracking performance and be stable in finite time instead of asymptotically stable. First, the third-order dynamics model and spacing strategy of the vehicle are given. The tracking performance of the vehicle formation is specified. Then, the control objective of the system is transformed by using the error transformation to obtain a new system. An improved sliding mode surface is designed for the transformed system. Furthermore, the universal approximation property of the neural network is utilised to overcome the parameter uncertainty in the system. The reconstruction error of neural network is handled by a robust term. In addition, the jittery vibration phenomenon of sliding mode control has been overcome. Finally, the finite-time stability of the system is analysed by constructing the Lyapunov function, simulations were performed to validate and compare with conventional control methods, simulation results show that the novel control method proposed in this paper is significantly faster than the conventional control method, validated the effectiveness of the method proposed in this paper.**

***Index Terms*—finite-time; sliding mode control; vehicle formation; neural network**

I. Introduction

IN recent years, accelerated urbanization has expanded the demand for Intelligent Transportation Systems (ITS)[1].

Vehicle formation system as an important part of the intelligent transport system is of great significance in improving traffic. Vehicle formation control is to control a single vehicle as a control model, and then control the whole formation. Vehicle formation control to dynamically simulate vehicle models, and design the controller. Vehicle formation improves the density of vehicles to slow down traffic congestion, increase the flow of vehicles, make traffic control simple, reduce the incidence of traffic accidents, and improve the safety of road driving[2].

Vehicle cooperative control is to enable multiple vehicles to travel smoothly in formation with the same state (speed as well as acceleration), with adjacent vehicles achieving the desired spacing at a steady state[3]. By reducing the inter-vehicle distance, the number of vehicles running on a section of the road is increased, and the utilization rate of the road is increased. It improves the traffic capacity of the intelligent transportation system and relieves the pressure of traffic congestion[4].

Most of the current research on dynamics modelling for formation vehicles has been on the dynamics of individual vehicles. In the current research results, vehicle models are usually classified into linear and non-linear models, which can be further classified into first-order, second-order[5] and third-order models[6]. The first-order model is the simplest kind of linear model describing the vehicle motion, with the velocity of the vehicle as the control input and the vehicle displacement as the only motion state. Although this model can simplify the controller design, the state of the formation in the actual travelling process is very complicated, and a single first-order model is far away from reality, which does not apply to the current research. The second-order model is by far the most widely used, and many important current theoretical results on vehicle formation control rely on the second-order model. [7] proposes a second-order model with acceleration as the control input and the velocity and displacement of the vehicle as the motion state[7], which provides a more accurate modelling of the formation vehicle. However, there are still some complex dynamics that cannot be described, such as the vehicle's engine mechanics and factors such as inertial delays. The third-order model can approximate the input-output behaviour of the dynamics in the vehicle dynamics system, with the addition of acceleration as a state to further characteristics of the real vehicle dynamics[8].

In formation control, various uncertainties as well as external disturbances are often encountered. And the sliding mode control has strong robustness to overcome these factors. [9] proposed a lateral control method using linear sliding mode control to make the formation spacing error minima[9]. [10] uses an integral sliding mode control method to propose a fixed pitch strategy controller, integrated consideration of vehicle interactions, spacing errors, and external disturbance[10]. [11] proposes a robust tracking controller based on terminal sliding modes to ensure formation

Manuscript received August 14, 2024; revised January 7, 2025. The research work was supported by the Fundamental Research Funds for the Liaoning Universities (LJ212410146025).

Dongyang Guo is a graduate student at the School of Electronic and Information Engineering, University of Science and Technology Liaoning, Anshan, 114051, China. (e-mail: guodongyang1@qq.com).

Zhao Zhang is an associate professor of School of Computer Science and Software Engineering, University of Science and Technology Liaoning, Anshan, 114051, China. (corresponding author, e-mail: zhangzhao333@hotmail.com).

Hongyan Zhou is a doctoral student of School of Electronic and Information Engineering, University of Science and Technology Liaoning, Anshan, 114051, China. (e-mail: zhou321yan@163.com).

Xue-Bo Chen is a professor of School of Electronic and Information Engineering, University of Science and Technology Liaoning, Anshan, 114051, China. (e-mail: xuebochen@126.com).

stability[11]. However, they don't specify spacing errors for formations. [12] uses linear sliding mode control to study the problem of formation control with a prescribed spacing error[12]. [13] addresses the prescribed spacing error of vehicle formations by designing distributed controllers to ensure the steady state performance of vehicle formations[13]. However, all of their controllers can only achieve asymptotically stable control, which is not enough for formation control.

Finite-time control has the advantages of fast response speed, high disturbance resistance and high control accuracy[14]. [15] proposes a finite time control method that allows for fast convergence of formation spacing errors, but only for second-order vehicle models[15]. [16] proposes controllers that keep the formation stable for a finite amount of time, but they ignore the queue stability of the formation[16].

In actual formation driving, there are often many uncertainties that affect the system parameters. As neural networks have strong nonlinear approximation ability and learning ability, they can counteract the negative effects of these uncertainties on system control, and open up a new way for the control of complex nonlinear systems[17]. Adaptive control of neural networks is a new method based on the basic principle of adaptive, combined with the characteristics and theories of neural networks, which simplifies the complexity of the design of purely adaptive control systems, and thus has received widespread attention in the field of intelligent control research.

Based on the above analyses, this paper addresses the vehicle formation provision tracking performance problem. The main innovations of this paper are concluded as follows:

(1) This paper addresses the prescribed spacing error of the third-order vehicle model and designs a novel control algorithm based on improved sliding mode control and neural network. The neural network is used to approximate the complex fuzzy dynamics in the control process, the adaptive term is used to overcome the external interference, and the robust term to overcome the reconstruction error of the neural network.

(2) The new control algorithm proposed in this paper can ensure that the vehicle formation is stable in finite time instead of asymptotically stable.

The paper is structured as follows: section 2 describes the vehicle model and control objectives of the formation system. Section 3 gives the design of the finite time controller. Section 4 verifies the controller by numerical simulation. Section 5 concludes the paper.

II. Problem Description

A. Vehicle dynamics modelling

In this paper, the vehicle formation structure is a Predecessor Following (PF) structure, which consists of a leader vehicle ($i=0$) and N following vehicles. As shown in Fig. 1, where $L_i(t)$, $v_i(t)$ and $a_i(t)$ denote the real-time position, velocity and acceleration of the vehicle i, respectively. $P_{d,i}$ represents the desired spacing between vehicles $i-1$ and i, the ideal distance between vehicles including the length of the vehicle as well as the safety distance required to start and stop the vehicle, e_i represents the error between the ideal spacing of vehicles $i-1$ and i with the actual spacing in the control, known as the spacing error. It is assumed that vehicles can communicate with each other while travelling, detecting the state information of adjacent vehicles, and that the communication channel is completely reliable.

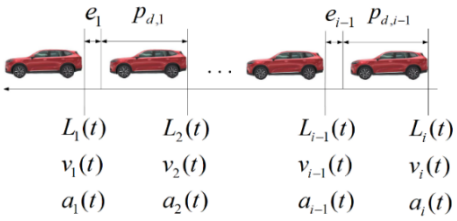

Fig. 1 Vehicle formation model

The model of the third-order dynamics of a single vehicle in a formation can be represented as

$$\begin{cases} \dot{L}_i(t) = v_i(t), \\ \dot{v}_i(t) = a_i(t) \\ \dot{a}_i(t) = -\dfrac{1}{m_i\partial}[P(v_i^2 + 2v_i\partial a_i) + f] + \dfrac{u_i(t)}{m_i\partial} - \dfrac{1}{\partial}a_i(t) + \omega_i(t) \end{cases} \tag{1}$$

where m_i is the mass of the vehicle i; ∂ is the engine time constant of the vehicle, assuming that all vehicles are of the same model and have the same engine time constant; $P = \dfrac{\varphi A_i \alpha}{2}$, P is the air resistance during travelling; φ is the density of air around the vehicle; A_i is the maximal cross-sectional area of vehicle i; α is the air resistance coefficient; f is the frictional resistance of the vehicle during travelling, to facilitate the calculations, define $f = \mu mg(\cos\theta + \sin\theta)$, μ is the wheel rolling resistance coefficient, θ is the gradient of the road travelled; $u_i(t)$ is the control input; $\omega_i(t)$ is a concentrated disturbance caused by weather versus roads.

B. quadratic spacing strategy

The stability of the formation is critical, and the key to controlling stability is to control the tracking performance of the vehicles in the formation, which is the spacing error between each vehicle. Common spacing strategies are fixed spacing strategies and variable spacing strategies[18].

This paper considers the vehicle length, the driver's reaction time, the vehicle's safety braking distance and the vehicle's speed to propose a variable quadratic spacing strategy. The ideal workshop distance is set as a quadratic function about the speed, so that the workshop spacing is automatically adjusted with the speed of the vehicle to obtain the ideal workshop spacing, with the expression as follows

$$e_i = L_{i-1} - L_i - q_{1,i} - q_2 - t_s v_i(t) - \frac{\zeta v_i^2(t)}{2a_n} \tag{2}$$

$$P_{d,i} = q_{1,i} + q_2 + t_s v_i(t) + \frac{\zeta v_i^2(t)}{2a_n} \tag{3}$$

where $\&_i(t) = L_{i-1} - L_i$ represents the actual distance between any two adjacent vehicles, $q_{1,i}$ denotes the length of vehicle i, q_2 denotes the given safety distance, t_s denotes the reaction time for braking or accelerating, $t_s v_i(t)$ denotes braking distance, ζ denotes a safety factor based on the external environment, a_n denotes the absolute value of the maximal deceleration.

C. control objective

The objective of this paper is to design an adaptive control algorithm, and the control objective is to use this control algorithm to control each vehicle in the formation. When the leader vehicle operates in an arbitrary state (speed as well as acceleration), the state of each follower vehicle can follow the leader vehicle for a finite time, and the spacing between two adjacent vehicles can reach a desired state, thus achieving the transient and steady-state performance of the formation. More specifically, the objective of the research in this paper is to design a controller $u_i(t)$ such that the

(1) Finite-time stability[19]: ensure that in a finite time, the spacing error of the formation can satisfy the regulations, and at the same time, the speed and acceleration of each vehicle can keep up with the leader vehicle.

$$\begin{cases} \lim\limits_{t\to T} \|e_i\| \le \Psi, \\ v_i(t) \to v_0(t) \\ a_i(t) \to a_0(t) \end{cases} \tag{4}$$

(2) Traffic flow stability[20]: when the formation is stable, the derivative $\frac{dD}{d\rho}$ of the traffic volume D with respect to the traffic density ρ is positive, $\frac{dD}{d\rho} > 0$.

D. prerequisite knowledge

Lemma 1[21] For a nonlinear system $\dot{x} = f(x,u)$, if there exists a positive definite function $V(x)$ and exist parameters $c > 0$ and $0 < \lambda < 1$ such that

$$\dot{V}(x) \le -cV^{\lambda}(x), t > 0 \tag{5}$$

Then the system is finite time stable. The time of convergence depends on the initial state $x(0) = x_0$, which is given by

$$T_x(x_0) \le \frac{V^{1-l}(x_0)}{c(1-l)} \tag{6}$$

Lemma 2[22] For a nonlinear system $\dot{x} = f(x,u)$, if there exists a positive definite function $V(x)$ and exist parameters $a, b > 0$ and $0 < r < 1$ such that

$$\dot{V}(x) \le -aV(x) - bV^r(x), t > 0 \tag{7}$$

Then the system is exponentially stable and faster finite time stable. The time of convergence depends on the initial state $x(0) = x_0$, which is given by

$$T_x(x_0) \le \frac{1}{a(1-r)} \ln \frac{aV^{1-r}(x_0) + b}{b} \tag{8}$$

Lemma 3[23] For a nonlinear function $f(x): R^n \to R$, there exists an ideal weight vector W and an arbitrarily small positive constant ε enabling the neural network to approximate $f(x)$ in the following way:

$$f(x) = W^T h(X) + \varepsilon \tag{9}$$

where $W \in \mathbb{R}^n$ is the ideal weight matrix of the output layer of the neural network, $\varepsilon \in \mathbb{R}$ is the reconstruction error of the neural network approximation, and $h(X)$ is the activation function.

III. Control Methods

A. system transformation

The system (1) is the vehicle dynamics model of the formation system, and the control of the vehicle system can only be dependent on the dynamics model, the control objective of this paper is to control the spacing error(2), so to facilitate the achievement of the control objective and to make the control inputs dependent on the spacing error(2), we choose the new state variable as:

$$\begin{cases} x_{1,i} = L_{i-1} - L_i - q_{1,i} - q_2 - t_s v_i(t) - \frac{\zeta v_i^2(t)}{2a_n} \\ x_{2,i} = v_{i-1} - v_i - t_s a_i(t) - \frac{\zeta v_i(t) a_i(t)}{a_n} \end{cases} \tag{10}$$

By deriving the new state variables and combining them with the vehicle dynamics model of the system(1), we can get the new system:

$$\begin{cases} \dot{x}_{1,i} = x_{2,i} \\ \dot{x}_{2,i} = -[t_s + \frac{\zeta v_i(t)}{a_n}][f(v_i, a_i) + \frac{u_i(t)}{m_i \partial} + \omega_i(t)] \end{cases} \tag{11}$$

where

$$f(v_i, a_i) = -\frac{P}{m_i \partial}[v_i^2(t) + 2v_i(t)\partial a_i(t)] - [t_s + \frac{\zeta v_i(t)}{a_n}]^{-1}[a_{i-1}(t) - a_i(t) - \frac{\zeta a_i^2(t)}{a_n}] - \frac{1}{m_i \partial} f - \frac{1}{\partial} a_i(t) \tag{12}$$

The control objective of this paper is to make

$$\lim_{t\to T} \|x_{1,i}\| \le \Psi \tag{13}$$

To simplify the calculation, we can transform the target so that the

$$x_{1,i} \in (\Psi_{\min}, \Psi_{\max}) \to F(x_{1,i}) \in (-\infty, +\infty)$$

that is

$$\begin{cases} \lim_{x_{1,i} \to \Psi_{\max}^-} F(x_{1,i}) = +\infty \\ \lim_{x_{1,i} \to \Psi_{\min}^+} F(x_{1,i}) = -\infty \end{cases} \tag{14}$$

where $\Psi_{\min} = -\Psi_{\max}$, for ease of calculation, we need to obtain a function of $x_{1,i}$ about $F(x_{1,i})$, which is calculated:

$$x_{1,i}=\frac{\Psi_{\max}e^{F(x_{1,i})}+\Psi_{\min}e^{-F(x_{1,i})}}{e^{F(x_{1,i})}+e^{-F(x_{1,i})}} \tag{15}$$

Continuing the calculation, the transformation function $F(x_{1,i})$ is derived as

$$F(x_{1,i})=\frac{1}{2}\ln(\frac{x_{1,i}-\Psi_{\min}}{\Psi_{\max}-x_{1,i}}) \tag{16}$$

In order to transform $x_{1,i}\in(\Psi_{\min},\Psi_{\max})$ to $F(x_{1,i})\in(-\infty,+\infty)$, we should choose the transformation function $F(x_{1,i})$ to be an invertible smooth singular function.

For ease of computation, we take the new state variable $y_{1,i}=F(x_{1,i})$, substitute it into equation (16) and derive it to obtain the following new system

$$\begin{cases}\dot{y}_{1,i}=y_{2,i}\\ \dot{y}_{2,i}=\dfrac{d^2F(x_{1,i})}{dx_{1,i}^{\ 2}}x_{2,i}^{\ 2}-\dfrac{dF(x_{1,i})}{dx_{1,i}}[t_s+\\ \qquad\dfrac{\zeta v_i(t)}{a_n}][f(v_i,a_i)+\dfrac{u_i(t)}{m_i\partial}+\omega_i(t)]\end{cases} \tag{17}$$

From equation (16), it follows that whenever $F(x_{1,i})\in(-\infty,+\infty)$, we get $x_{1,i}\in(\Psi_{\min},\Psi_{\max})$, which means that the prescribed properties of $x_{1,i}$ are satisfied whenever $y_{1,i}$ is bounded. Therefore, the control objective can be achieved by controlling the new system(17).

B. slide mode control

Vehicle formation systems suffer from model uncertainty as well as external disturbances. Due to the specification of the tracking performance, in order to achieve the control objective in a finite time, based on the converted system (17), a modified sliding mode surface is designed

$$s_i=y_{2,i}+\mathcal{E}\mathcal{M}(y_{1,i}) \tag{18}$$

where

$$\mathcal{M}(y_{1,i})=\begin{cases}\left|y_{1,i}\right|^{\gamma}\operatorname{sgn}\left(y_{1,i}\right) & s=0\ or\ s\neq0,\left|y_{1,i}\right|>\upsilon\\ l_1y_{1,i}+l_2\left|y_{1,i}\right|^{2}\operatorname{sgn}\left(y_{1,i}\right) & s\neq0,\left|y_{1,i}\right|<\upsilon\end{cases}$$

where $\frac{1}{2}<\gamma<1$, and γ are fractions with positive odd numerators and denominators, $\upsilon>0$ is a small positive number, $l_1=(2-\gamma)\upsilon^{\gamma-1}$, $l_2=(\gamma-1)\upsilon^{\gamma-2}$, sgn(•) are signed functions.

When the slide mode surface $s_i=0$, $y_{2,i}=-\mathcal{E}\mathcal{M}(y_{1,i})$.

$$y_{2,i}=\begin{cases}-\mathcal{E}\left|y_{1,i}\right|^{\gamma}\operatorname{sgn}\left(y_{1,i}\right) & s=0\ or\ s\neq0,\left|y_{1,i}\right|>\upsilon\\ -\mathcal{E}l_1y_{1,i}-\mathcal{E}l_2\left|y_{1,i}\right|^{2}\operatorname{sgn}\left(y_{1,i}\right) & s\neq0,\left|y_{1,i}\right|<\upsilon\end{cases}$$

When $\left|y_{1,i}\right|<\upsilon$, $y_{2,i}=-\mathcal{E}l_1y_{1,i}-\mathcal{E}l_2\left|y_{1,i}\right|^{2}\operatorname{sgn}\left(y_{1,i}\right)$ has a faster convergence rate than $y_{2,i}=-\mathcal{E}\left|y_{1,i}\right|^{\gamma}\operatorname{sgn}\left(y_{1,i}\right)$. This indicates that the convergence rate of the improved slip mode surface is improved.

Derivation of the sliding mode surface (18) yields

$$\begin{aligned}\dot{s}_i&=\dot{y}_{2,i}+\mathcal{E}\dot{\mathcal{M}}(y_{1,i})\\ &=\mathcal{E}\dot{\mathcal{M}}(y_{1,i})+\frac{d^2F(x_{1,i})}{dx_{1,i}^{\ 2}}x_{2,i}^{\ 2}-\frac{dF(x_{1,i})}{dx_{1,i}}[t_s+\\ &\quad\frac{\zeta v_i(t)}{a_n}][f(v_i,a_i)+\frac{u_i(t)}{m_i\partial}+\omega_i(t)]\end{aligned} \tag{19}$$

where

$$\dot{\mathcal{M}}(y_{1,i})=\begin{cases}\gamma\left|y_{1,i}\right|^{\gamma-1}\dot{y}_{1,i} & s=0\ or\ s\neq0,\left|y_{1,i}\right|>\upsilon\\ l_1\dot{y}_{1,i}+2l_2\left|y_{1,i}\right|\dot{y}_{1,i} & s\neq0,\left|y_{1,i}\right|<\upsilon\end{cases}$$

choosing the sliding mode to be $\mathcal{M}(y_{1,i})$, rather than $\left|y_{1,i}\right|^{\gamma}\operatorname{sgn}\left(y_{1,i}\right)$, can avoid the singularity problem of $s\neq0,y_{1,i}=0$ or $y_{2,i}=0$. Moreover, its derivative is a continuous function.

Remark 1 Conventional sliding mode control, because of discontinuity in the control inputs, sgn(•) causes the well-known phenomenon of jitter. We will therefore use the saturation function (20) instead of sgn(•), where η is a small positive number indicates the thickness of the sliding mode boundary layer.

$$sat(s)=\begin{cases}1 & s>\eta\\ ks,k=\dfrac{1}{\eta} & |s|\le\eta\\ -1 & s<-\eta\end{cases} \tag{20}$$

C. neural network approximation

Neural networks have universal approximations, in applications, they are often used to estimate nonlinear dynamics and functions where uncertainty exists. Since there is some uncertainty in the system (17), $x_{1,i}$ and $x_{2,i}$ are measurable, we use RBF neural networks to approximate them

$$\begin{aligned}G_i(X)=&\frac{d^2F(x_{1,i})}{dx_{1,i}^{\ 2}}x_{2,i}^{\ 2}[\frac{dF(x_{1,i})}{dx_{1,i}}(t_s+\frac{\zeta v_i(t)}{a_n})]^{-1}+\\ &\mathcal{E}\dot{\mathcal{M}}(y_{1,i})[\frac{dF(x_{1,i})}{dx_{1,i}}(t_s+\frac{\zeta v_i(t)}{a_n})]^{-1}-f(v_i,a_i)\end{aligned} \tag{21}$$

According to the universal approximation property of neural networks, the unknown continuous function $G_i(X)$ can be rewritten as

$$G_i(X)=W_i^Th(X_i)+\varepsilon \tag{22}$$

where $X_i=[x_{1,i},x_{2,i}]$ is the input of the neural network, $W\in\mathbb{R}^n$ is the desired weights of the output layer of the neural network which can be adjusted according to the adaptive law given later, $\varepsilon\in\mathbb{R}^n$ is the reconstruction error of the neural network, and the activation function is chosen as Gaussian function $h(X)=e^{(\frac{\|X_i-c_i\|^2}{2b_i^2})}$, where $i=1,...,m$, m is the number of nodes in the hidden layer, c_i and b_i are constants, $h(\bullet)<\bar{h}$, $\bar{h}$ are positive numbers.

Assumption 1 In the neural network approximation

process, it is assumed that the ideal weights W and the reconstruction error ε are bounded, which satisfies $\|W\| \le w_m, \varepsilon \le \varepsilon_m$. Since the neural network is unknown, we use $\widehat{W}$ as an estimate of the ideal weights W. Define $\widetilde{W} = W - \widehat{W}$ as the neural network weights estimation error.

D. finite-time controller design

The controller of the system (17) is designed as follows:

$$u_i = m_i\partial\{\frac{k_n s + k_m \operatorname{sgn}(s)}{[t_s + \frac{\zeta v_i(t)}{a_n}]\frac{dF(x_{1,i})}{dx_{1,i}}} - \omega_i(t) + k_p \operatorname{sgn}(s) + \widehat{W}^T h(X_i) + \sigma \operatorname{sgn}(s)\} \tag{23}$$

where k_m, k_n, and k_p are all positive numbers, $\sigma_i > 0$ is an adaptive variable, $\widehat{\sigma_i}$ is used as an estimate of σ_i. $\widetilde{\sigma_i} = \sigma_i - \widehat{\sigma_i}$ is defined as the estimation error of the adaptive variable. Since the reconstruction error of neural networks is unavoidable, in many literature the reconstruction error of neural networks is treated as a known perturbation and needs to be computed in advance. In this paper, a robust term $k_p \operatorname{sgn}(s)$ is proposed to counteract the reconstruction error, which reduces the impact of the reconstruction error on the performance of the system without the need to be computed in advance.

The neural network's weights adaptive law $\widehat{W}$ is

$$\dot{\widehat{W}}_i = \chi s_i [t_s + \frac{\zeta v_i(t)}{a_n}]\frac{dF(x_{1,i})}{dx_{1,i}} h(X) \tag{24}$$

The adaptive law $\hat{\sigma}$ is

$$\dot{\widehat{\sigma}}_i = -s_i [t_s + \frac{\zeta v_i(t)}{a_n}]\frac{dF(x_{1,i})}{dx_{1,i}} \tag{25}$$

E. stability analysis

In order to ensure that the designed controller can satisfy the control requirements of the whole system, we use the Lyapunov theory to prove the whole system. The following theorem proves the stability results and performance of the proposed controller.

Theorem 1 For a vehicle formation system with PF structure, considering a single vehicle dynamics model (1), combining the vehicle spacing strategy (2), using the transformed system (17), designing an adaptive controller (23) based on the improved sliding modal surface (18) and the neural network (21), and combining the adaptive laws (24) and (25), the tracking control of the formation system can be achieved and the system is guaranteed to be stable in finite time. The system is stable for a finite time, the sliding mode surface s_i can converge to zero in a finite time and the spacing error can satisfy the regulations:

$$\lim_{t \to T} \|e_i\| \le \Psi$$

Proof: choose the following Lyapunov function:

$$V_i = \frac{1}{2} s_i^2 + \frac{1}{2\chi} \widetilde{W}_i^T \widetilde{W}_i + \frac{1}{2} \tilde{\sigma}^2 \tag{26}$$

Derivation of (26) yields:

$$\dot{V}_i = s_i \dot{s}_i + \frac{1}{\chi} \widetilde{W}_i^T \dot{\widetilde{W}}_i + \tilde{\sigma}\dot{\tilde{\sigma}} \tag{27}$$

where

$$s_i \dot{s}_i = s_i \{\mathcal{E}\mathcal{M}(\dot{y}_{1,i}) + \frac{d^2 F(x_{1,i})}{dx_{1,i}^2} x_{2,i}^2 - \frac{dF(x_{1,i})}{dx_{1,i}}[t_s + \frac{\zeta v_i(t)}{a_n}][f(v_i, a_i) + \frac{u_i(t)}{m_i\partial} + \omega_i(t)]\} \tag{28}$$

$$\frac{1}{\chi} \widetilde{W}_i^T \dot{\widetilde{W}}_i = \frac{1}{\chi} \widetilde{W}_i^T (\dot{W} - \dot{\widehat{W}}) = -\frac{1}{\chi} \widetilde{W}_i^T \dot{\widehat{W}} \tag{29}$$

thus

$$\begin{aligned} \dot{V}_i &= s_i \dot{s}_i + \frac{1}{\chi} \widetilde{W}_i^T \dot{\widetilde{W}}_i + \tilde{\sigma}\dot{\tilde{\sigma}} \\ &= s_i \{\frac{d^2 F(x_{1,i})}{dx_{1,i}^2} x_{2,i}^2 + \mathcal{E}\mathcal{M}(\dot{y}_{1,i}) - \frac{dF(x_{1,i})}{dx_{1,i}}[t_s + \frac{\zeta v_i(t)}{a_n}][f(v_i, a_i) + \frac{u_i(t)}{m_i\partial} + \omega_i(t)]\} - \frac{1}{\chi} \widetilde{W}_i^T \dot{\widehat{W}} - \tilde{\sigma}\dot{\tilde{\sigma}} \\ &= s_i \frac{dF(x_{1,i})}{dx_{1,i}}[t_s + \frac{\zeta v_i(t)}{a_n}]\{-f(v_i, a_i) - \frac{u_i(t)}{m_i\partial} - \omega_i(t) + \frac{\frac{d^2 F(x_{1,i})}{dx_{1,i}^2} x_{2,i}^2 + \mathcal{E}\mathcal{M}(\dot{y}_{1,i})}{\frac{dF(x_{1,i})}{dx_{1,i}}[t_s + \frac{\zeta v_i(t)}{a_n}]}\} - \frac{1}{\chi} \widetilde{W}_i^T \dot{\widehat{W}} - \tilde{\sigma}\dot{\tilde{\sigma}} \end{aligned} \tag{30}$$

Combining equations (21) and (22), it is obtained using neural network approximation:

$$G_i(X) = (\widetilde{W} + \widehat{W})h(X) + \varepsilon \tag{31}$$

Substituting equation (31) into equation (27) yields

$$\dot{V}_i = s_i \frac{dF(x_{1,i})}{dx_{1,i}}[t_s + \frac{\zeta v_i(t)}{a_n}]\{-\frac{u_i(t)}{m_i\partial} - \omega_i(t) + (\widetilde{W} + \widehat{W})h(X) + \varepsilon\} - \frac{1}{\chi} \widetilde{W}_i^T \dot{\widehat{W}} - \tilde{\sigma}\dot{\tilde{\sigma}} \tag{32}$$

Substituting the controller (23) into equation (32) yields

$$\dot{V}_i = s_i \frac{dF(x_{1,i})}{dx_{1,i}}[t_s + \frac{\zeta v_i(t)}{a_n}]\{\widetilde{W}^T h(X) + \varepsilon - k_p \operatorname{sgn}(s) - \frac{k_n s + k_m \operatorname{sgn}(s)}{[t_s + \frac{\zeta v_i(t)}{a_n}]\frac{dF(x_{1,i})}{dx_{1,i}}} - \sigma \operatorname{sgn}(s)\} - \frac{1}{\chi} \widetilde{W}_i^T \dot{\widehat{W}} - \tilde{\sigma}\dot{\tilde{\sigma}} \tag{33}$$

Substituting the adaptive laws (24) and (25) into (33)yields

$$\begin{aligned} \dot{V}_i &= -k_n s_i^2 - k_m s_i \operatorname{sgn}(s_i) + s_i \frac{dF(x_{1,i})}{dx_{1,i}}[t_s + \frac{\zeta v_i(t)}{a_n}]\{\widetilde{W}^T h(X) + \varepsilon - k_p \operatorname{sgn}(s)\} - \frac{1}{\chi} \widetilde{W}_i^T \chi s_i [t_s + \frac{\zeta v_i(t)}{a_n}]\frac{dF(x_{1,i})}{dx_{1,i}} h(X) \\ &= -k_n s_i^2 - k_m s_i \operatorname{sgn}(s_i) + s_i \frac{dF(x_{1,i})}{dx_{1,i}}[t_s + \frac{\zeta v_i(t)}{a_n}][\varepsilon - k_p \operatorname{sgn}(s) - \hat{\sigma} \operatorname{sgn}(s_i)] \end{aligned} \tag{34}$$

In equation (34), $k_p \operatorname{sgn}(s)$ is the robust term to counteract the reconstruction error ε of the neural network approximation, thus

$$\begin{aligned} \dot{V}_i &\le -k_n s_i^2 - k_m s_i \operatorname{sgn}(s_i) \\ &\le -k_n s_i^2 - k_m |s_i| \end{aligned} \tag{35}$$

Thus, it can be shown that the system is consistent and eventually bounded, and we can know $\left|\widetilde{W}^T h(X)\right| \le \tau$, τ is a small constant. Next, prove finite-time stability. The Lyapunov function is set to be

$$V_s = \frac{1}{2} s_i^2 \tag{36}$$

The derivation of this gives

$$\begin{aligned} \dot{V}_i &= s_i \dot{s}_i \\ &= s_i \{ \frac{d^2 F(x_{1,i})}{dx_{1,i}^2} x_{2,i}^2 + \mathcal{E}\dot{\mathcal{M}}(y_{1,i}) - \frac{dF(x_{1,i})}{dx_{1,i}} [t_s + \frac{\zeta v_i(t)}{a_n}] \\ &\quad [f(v_i, a_i) + \frac{u_i(t)}{m_i \partial} + \omega_i(t)] \} \\ &= s_i \frac{dF(x_{1,i})}{dx_{1,i}} [t_s + \frac{\zeta v_i(t)}{a_n}] \{ -\frac{u_i(t)}{m_i \partial} - \omega_i(t) + (\widetilde{W} + \\ &\quad \widehat{W}) h(X) + \varepsilon \} \end{aligned} \tag{37}$$

Substituting the controller (23) yields

$$\begin{aligned} \dot{V}_s &= -k_n s_i^2 - k_m |s_i| + s_i \frac{dF(x_{1,i})}{dx_{1,i}} [t_s + \frac{\zeta v_i(t)}{a_n}] \{ \widetilde{W} h(X) + \\ &\quad \varepsilon - k_p \operatorname{sgn}(s_i) - \sigma \operatorname{sgn}(s_i) \} \\ &\le -k_n s_i^2 + s_i \frac{dF(x_{1,i})}{dx_{1,i}} [t_s + \frac{\zeta v_i(t)}{a_n}] [\widetilde{W} h(X) - \\ &\quad \sigma \operatorname{sgn}(s_i)] \end{aligned} \tag{38}$$

Recall that equation (16) shows that there exists a positive number $\phi > 1$ satisfying $\frac{dF(x_{1,i})}{dx_{1,i}} > \phi > 0$, and there exists a small positive number $\&$ satisfying $t_s + \frac{\zeta v_i(t)}{a_n} > \& > 0$. Knowing $\sigma > \tau$, set $\beta = \sigma - \tau > 0$. Thus

$$\dot{V}_s \le -k_n s_i^2 - \phi \& \beta |s_i| \le -2k_n V_s - \phi \& \beta V_s^{\frac{1}{2}} \tag{39}$$

Using Lemma 2, we conclude that s is finite time stable and the stability time function T satisfies

$$T \le \frac{2}{a} \ln \frac{a V^{\frac{1}{2}} + b}{b} \tag{40}$$

where $a = 2k_n$, $b = \phi \& \beta$, therefore, it can be shown that the system can reach stability in finite time, and it can be shown that $y_{1,i}$ is bounded, so we get $x_{1,i} \in (\Psi_{\min}, \Psi_{\max})$, which satisfies the control objective of the system.

F. traffic flow stability

Theorem 2 For a vehicle formation system with a PF structure, considering a single vehicle dynamics model (1), combined with a vehicle spacing strategy (2), the stability of the traffic flow of the whole convoy can be ensured.

Proof:

$$\rho = \frac{N}{L} = \frac{D}{\overline{V_S}} \tag{41}$$

where ρ is the traffic density, N is the number of vehicles in the road section, L is the length of the road section, D is the amount of traffic on the lane (flow rate), $\overline{V}_S$ is the average speed of vehicles in the interval. Assuming that the formation system arrives at a steady state, the safety distance of vehicles and the average speed arrives at the same, take the length of the road section L as $L = q_{1,i} + q_2 + t_s v + \frac{\zeta v^2}{2a_n}$, the vehicles within the road section N as 1, the average speed $\overline{V}_S$ as v, the traffic density as

$$\rho = \frac{1}{q_{1,i} + q_2 + t_s v + \frac{\zeta v^2}{2a_n}} \tag{42}$$

The function v can be introduced and substituted into the flow rate $D = \rho v$ to get

$$\begin{aligned} D &= \rho v \\ &= \rho \left(\sqrt{ (\frac{1}{\rho} - q_{1,i} - q_2) \frac{2a_n}{\zeta} + (\frac{t_s a_n}{\zeta})^2 } - \frac{t_s a_n}{\zeta} \right) \end{aligned} \tag{43}$$

Derivation of this yields:

$$\begin{aligned} \dot{D} &= \sqrt{ (\frac{1}{\rho} - q_{1,i} - q_2) \frac{2a_n}{\zeta} + (\frac{t_s a_n}{\zeta})^2 } - \frac{t_s a_n}{\zeta} - \\ &\quad \frac{a_n}{\rho \zeta \sqrt{ (\frac{1}{\rho} - q_{1,i} - q_2) \frac{2a_n}{\zeta} + (\frac{t_s a_n}{\zeta})^2 }} \end{aligned} \tag{44}$$

From equation (44), it can be shown that the derivative $\dot{D}$ is 0 when the critical density

$$\rho_s = \frac{1}{2(q_{1,i} + q_2) + t_s \sqrt{\frac{2(q_{1,i} + q_2) a_n}{\zeta}}}$$

and $\rho > \rho_s$, so $\dot{D} > 0$, the formation reaches traffic flow stability.

IV. Simulation Experiment

To verify the effectiveness of the proposed control algorithm, the vehicle formation is simulated in MATLAB environment. In the simulation, the vehicle formation consists of a leader vehicle and four follower vehicles travelling in a straight lane. Set the leader vehicle's initial states to be $L_0(0) = 0$, $v_0(0) = 0$. With no collision risk guaranteed, the initial states of the four following vehicles are $L_i(0) = [-24; -48; -72; -96]$, $v_i(0) = [0; 0; 0; 0]$, $a_i(0) = [0; 0; 0; 0]$.

The time of the simulation experiment is set to 80 s, assuming that each vehicle has the same parameters, where the parameters of the vehicle are set as follows[24]: mass of the vehicle m_i = 1600 kg, air resistance P = 0.414, running resistance of the vehicle f = 240, length of the vehicle $q_{l,i}$ = 4 m, ideal safety distance q_2 = 7 m, safety factor of the external environment of the vehicle ζ = 0.2, braking or acceleration reaction time t_s = 0.12 s, maximum deceleration of the possible value a_n =7, and concentrated disturbance $\omega_i(t) = 0.1\cos(t)$. The parameters of the controller are shown in Table I.

TABLE I
CONTROLLER PARAMETERS

Ψ_{min}	Ψ_{max}	γ	υ
−0. 05	0. 05	7 / 9	0. 1
ε	k_n	k_m	k_p
0. 03	0. 03	1	10

The acceleration of the leader vehicle is set to

$$a_0 = \begin{cases} 0.5t\ m/s^2 & 0 \le t < 4s \\ 2t\ m/s^2 & 4 \le t < 8s \\ -0.5t + 6\ m/s^2 & 8 \le t \le 12s \\ 0\ m/s^2 & t > 12 \end{cases}$$

The leader's acceleration, velocity, and displacement are shown in Fig. 2-4. The leader's acceleration increases and then decreases to zero after 12 s, and its velocity settles to 16 m/s after 12 s.

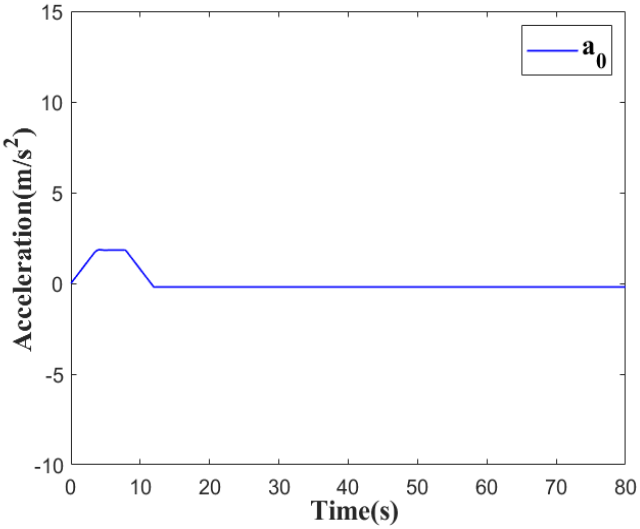

Fig.2 Leader car acceleration

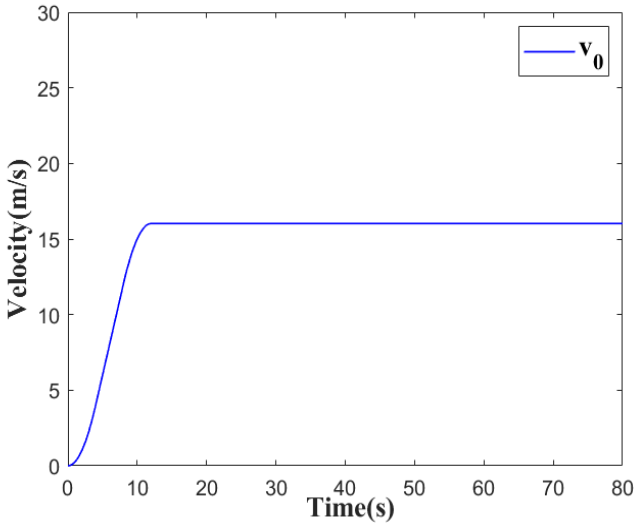

Fig.3 Leader car speed

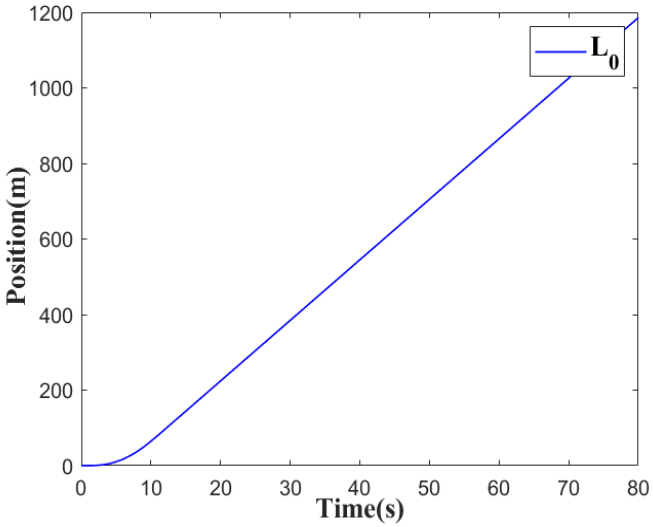

Fig.4 Leader car displacement

A. *simulation results*

This paper designed the control algorithm simulation results are shown in Figs. 5-10. Fig. 5 shows the displacement relationship of the formation vehicle, which can be intuitively seen that the displacement of the follower vehicle always follows the leader vehicle. Fig. 6 shows the velocity relationship of the formation vehicle, and Fig. 7 shows the acceleration relationship of the formation vehicle. After the system is stable, the velocity and acceleration can be consistent with the leader vehicle. Fig. 8 reflects the information of the displacement error of the formation, the displacement error will be adjusted with the speed of the vehicles, and finally kept at about 14 m, that is, the inter-vehicle distance between two adjacent vehicles will be kept at about 14 m. Fig. 9 reflects the information of the slip mode surface, which converges to zero. Fig. 10 reflects the spacing error information of the formation, the formation system can reach the specified spacing error within 2 s, and then continue to converge, the analysis shows that the RBF neural network has very good real-time performance. The spacing error can be converged to 0 around 6 s, to achieve the stability of the whole formation.

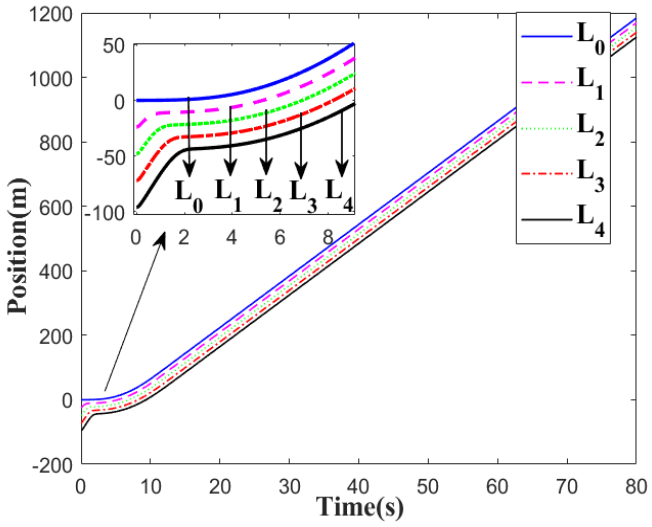

Fig.5 Displacement of formation vehicles

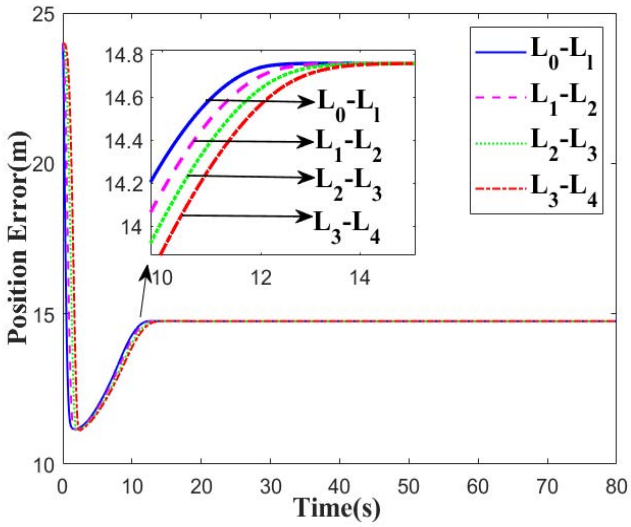

Fig.8 Displacement error of formation vehicles

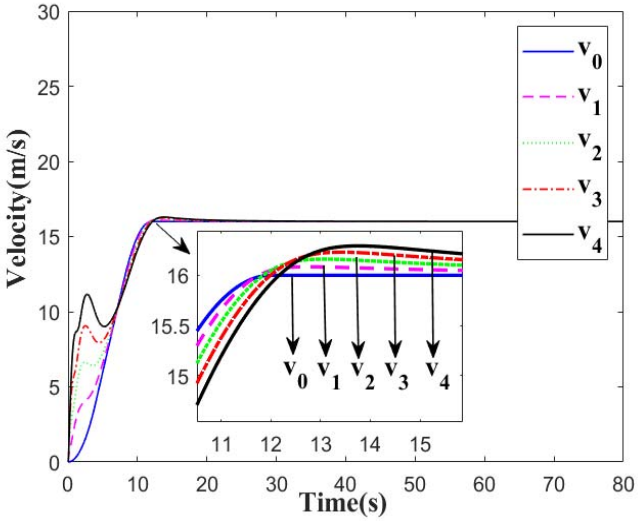

Fig.6 Speed of formation vehicles

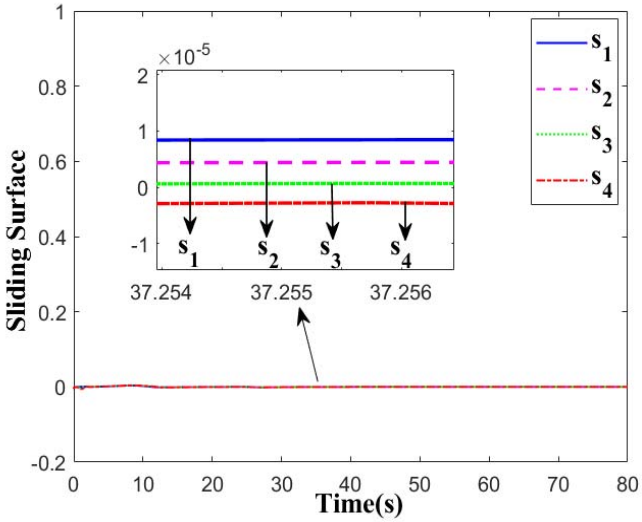

Fig.9 Surface of sliding mode

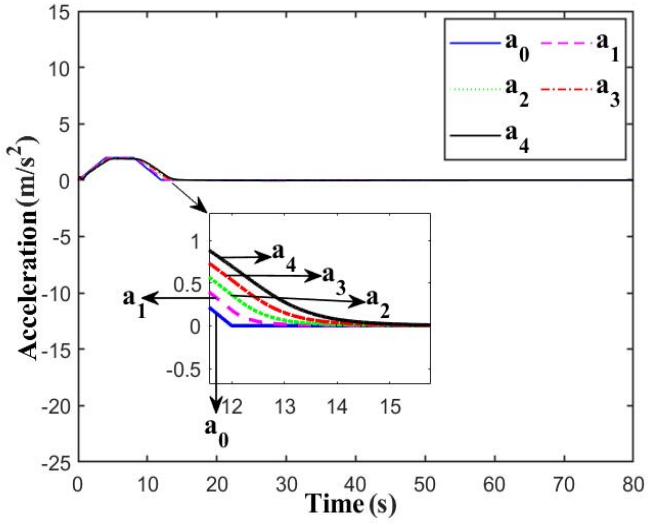

Fig.7 Acceleration of formation vehicles

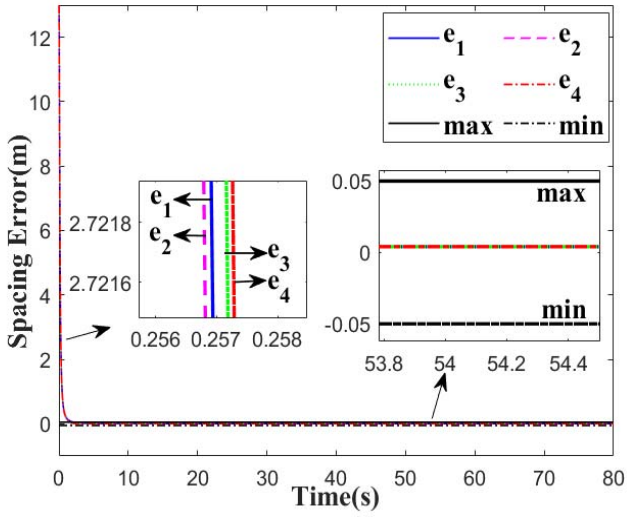

Fig.10 Spacing error of formation vehicles

B. comparative experiment

In order to further illustrate the performance advantages of the novel control algorithm designed in this paper, simulations are compared with literature[19], which does not specify the spacing error and uses a conventional sliding mode function. Set the sliding mode function as $s_i = e_i(t) + csign(e_i(t))|e_i(t)|^{\frac{1}{2}}$, the controller is

$$u_i = m_i\partial\{\frac{k_n s + k_m \operatorname{sgn}(s) + f(v_i, a_i)}{t_s + \frac{\zeta v_i(t)}{a_n}} - \omega_i(t) + \frac{1}{m_i\partial}[P(v_i^2 + 2v_i\partial a_i) + f] + \frac{1}{\partial}a_i(t)\} \quad (45)$$

The initial conditions are consistent with this paper, the simulation results are shown in Figs. 11-16. Fig. 11 shows the displacement relationship of the formation vehicles, which can be seen intuitively that the follower vehicle spends more time following the leader vehicle. Figs. 12-13 are the speed and acceleration relationship of the formation vehicles. Fig. 14 is the vehicle displacement error. Fig. 15 is the spacing error information of the formation vehicles. Fig. 16 is the information of the sliding mode surface, and analysis can be obtained that the spacing error can be converted to 0 around 16 s. Comparing Figs. 5-10, it can be obtained that the control algorithm proposed in this paper converges faster than the conventional finite-time sliding-mode control with the unspecified spacing error by about 10 s, which can better achieve the formation control requirements.

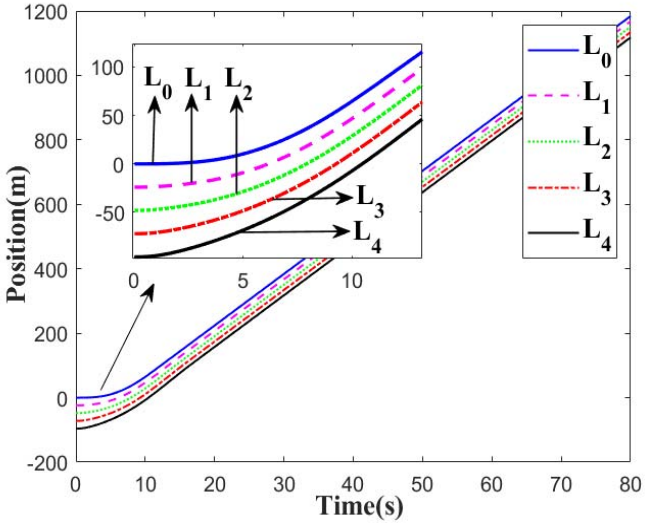

Fig.11 Displacement of formation vehicles

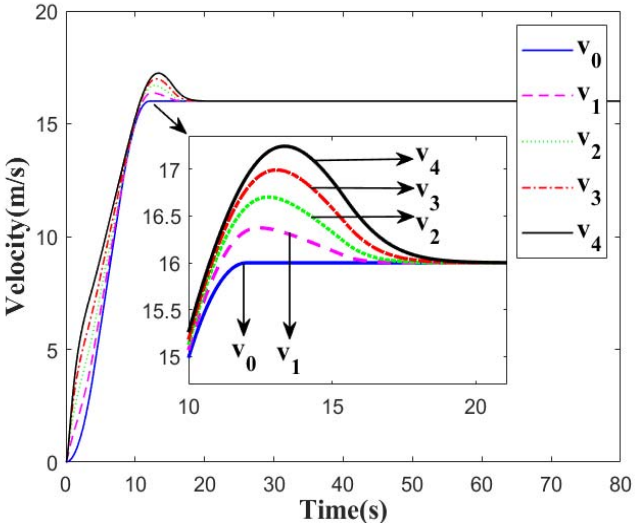

Fig.12 Speed of formation vehicles

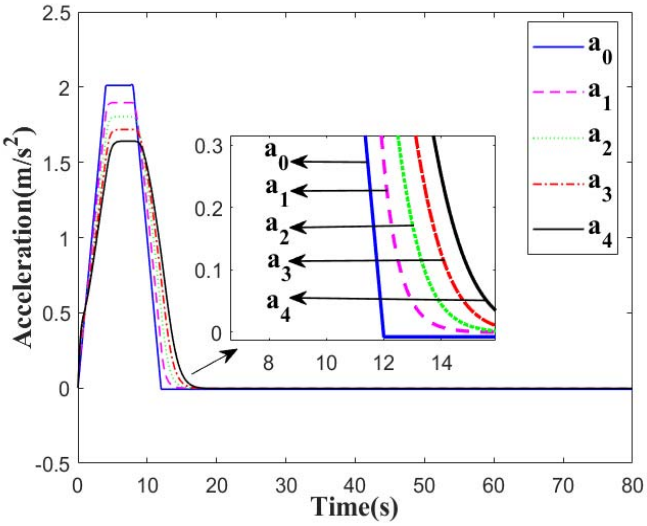

Fig.13 Acceleration of formation vehicles

V. Conclusion

This paper investigates the vehicle formation control problem and proposes a novel control algorithm. Vehicle formations can reach a steady state in a finite time and satisfy the specified tracking performance. Using a combination of improved sliding modes and neural networks to improve the performance of the formation system. The bounded perturbation and reconstruction errors of the neural networks are compensated with adaptive laws and robust terms, and the jitter phenomenon of the sliding modes is improved. Finally, the validity of the proposed method is verified by simulation. In this paper, during the control of vehicle formation, the system communication channel is completely reliable, without considering the possible interference. In the future, vehicle formation control with incompletely reliable communication channels is worth investigating.

References

[1] S. Chu, and A. Majumdar, "Opportunities and challenges for a sustainable energy future," *Nature,* vol. 488, no. 7411, pp. 294-303, 2012/08/01, 2012.

[2] B. Wu, and H. Tang, "A Summary of Research on Longitudinal Security Control of Intelligent Vehicle Plato," *Agricultural Equipment & Vehicle Engineering,* vol. 59, no. 7, pp. 6, 2021.

[3] G. Guo, Q. Zhang, and Z. Y. Gao, "Finite-time Fixed Configuration Formation Control of Intelligent Vehicles with Prescribed Transient and Steady-state Performance," *China Journal of Highway and Transport,* vol. 35, no. 3, pp. 28-42, 2022-03-20, 2022.

[4] C. Hong, H. Shan, M. Song *et al.*, "A Joint Design of Platoon Communication and Control Based on LTE-V2V," *IEEE Transactions on Vehicular Technology,* vol. 69, no. 12, pp. 15893-15907, 2020.

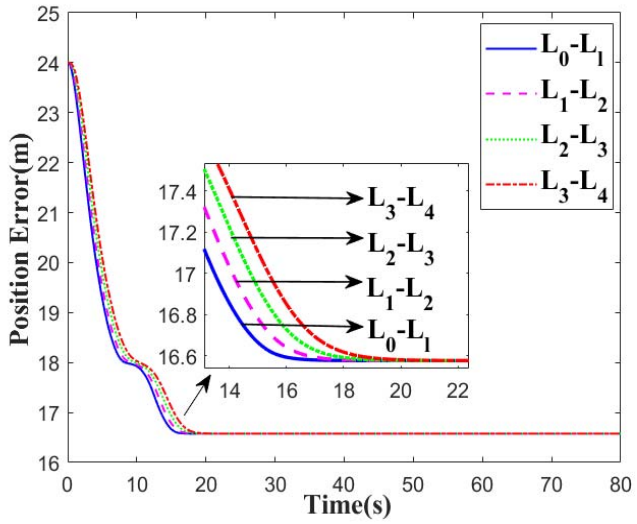

Fig.14 Displacement error of formation vehicles

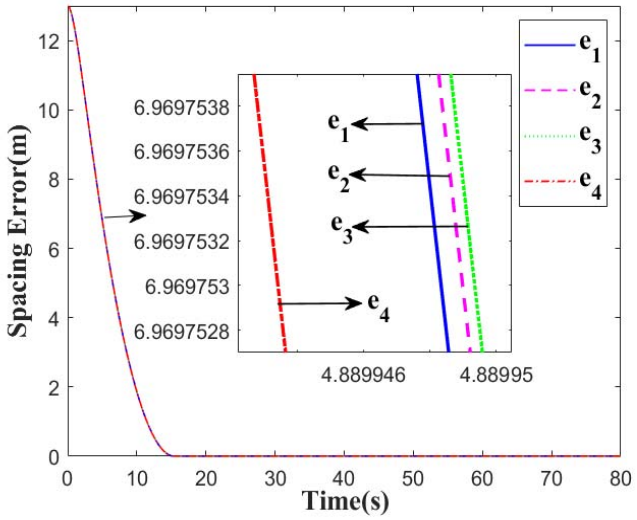

Fig.15 Spacing error of formation vehicles

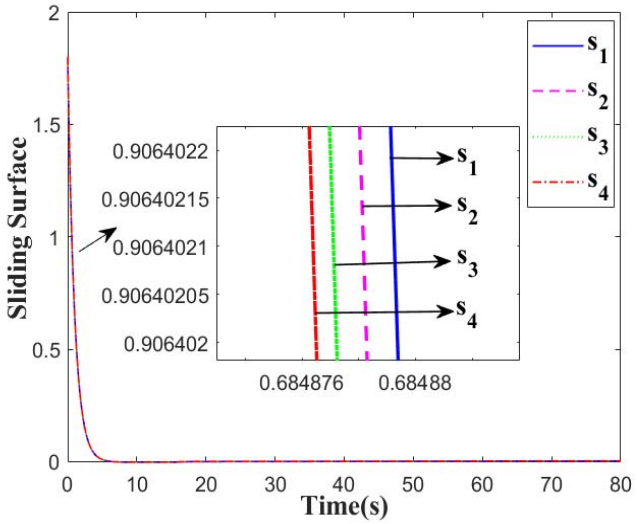

Fig.16 Surface of sliding mode

[5] X. Guo, J. Wang, F. Liao *et al.*, "Distributed Adaptive Sliding Mode Control Strategy for Vehicle-Following Systems With Nonlinear Acceleration Uncertainties," *IEEE Transactions on Vehicular Technology,* vol. 66, no. 2, pp. 981-991, 2017.

[6] J. Sawant, U. Chaskar, and D. Ginoya, "Robust Control of Cooperative Adaptive Cruise Control in the Absence of Information About Preceding Vehicle Acceleration," *IEEE Transactions on Intelligent Transportation Systems,* vol. 22, no. 9, pp. 5589-5598, 2021.

[7] X. G. Guo, W. D. Xu, J. L. Wang *et al.*, "BLF-Based Neuroadaptive Fault-Tolerant Control for Nonlinear Vehicular Platoon With Time-Varying Fault Directions and Distance Restrictions," *IEEE Transactions on Intelligent Transportation Systems,* vol. 23, no. 8, pp. 12388-12398, 2022.

[8] X. H. Yu, and G. Guo, "A general variable time hesdway policy in platoon control," *Acta Automatica Sinica*, no. 7, pp. 9, 2019.

[9] X. Ji, X. He, C. Lv *et al.*, "Adaptive-neural-network-based robust lateral motion control for autonomous vehicle at driving limits," *Control Engineering Practice,* vol. 76, pp. 41-53, 2018/07/01/, 2018.

[10] Y. Li, C. Tang, S. Peeta *et al.*, "Integral-Sliding-Mode Braking Control for a Connected Vehicle Platoon: Theory and Application," *IEEE Transactions on Industrial Electronics,* vol. 66, no. 6, pp. 4618-4628, 2019.

[11] Y. Wu, L. Wang, J. Zhang *et al.*, "Path Following Control of Autonomous Ground Vehicle Based on Nonsingular Terminal Sliding Mode and Active Disturbance Rejection Control," *IEEE Transactions on Vehicular Technology,* vol. 68, no. 7, pp. 6379-6390, 2019.

[12] G. Guo, and D. Li, "Adaptive Sliding Mode Control of Vehicular Platoons With Prescribed Tracking Performance," *IEEE Transactions on Vehicular Technology,* vol. 68, no. 8, pp. 7511-7520, 2019.

[13] C. K. Verginis, C. P. Bechlioulis, D. V. Dimarogonas *et al.*, "Robust Distributed Control Protocols for Large Vehicular Platoons With Prescribed Transient and Steady-State Performance," *IEEE Transactions on Control Systems Technology,* vol. 26, no. 1, pp. 299-304, 2018.

[14] Y. Liu, Y. W. Jing, X. P. Liu *et al.*, "Survey on finite-time control for nonlinear systems," *Control Theory and Technology,* vol. 37, no. 1, pp. 12, 2020.

[15] L. L. Yu, Z. X. Kuang, Z. J. Wang *et al.*, "Intelligent vehicle platoon lateral and longitudinal control based on finite-time sliding mode control," *Control Theory and Technology,* vol. 38, no. 8, pp. 1299-1312, 2021.

[16] A. Coppola, D. G. Lui, A. Petrillo *et al.*, "Distributed Fixed-Time Leader-Tracking Control for Heterogeneous Uncertain Autonomous Connected Vehicles Platoons." pp. 554-559.

[17] D. Elbrächter, D. Perekrestenko, P. Grohs *et al.*, "Deep Neural Network Approximation Theory," *IEEE Transactions on Information Theory,* vol. 67, no. 5, pp. 2581-2623, 2021.

[18] G. Guo, P. Li, and L. Y. Hao, "A New Quadratic Spacing Policy and Adaptive Fault-Tolerant Platooning With Actuator Saturation," *IEEE Transactions on Intelligent Transportation Systems,* vol. 23, no. 2, pp. 1200-1212, 2022.

[19] G. Guo, and Z. W. Zhao, "Finite-time terminal sliding mode control of connected vehicle platoons," *Control Theory and Technology,* vol. 40, no. 1, pp. 149-159, 2023.

[20] G. Guo, P. Li, and L. Y. Hao, "Adaptive Fault-Tolerant Control of Platoons With Guaranteed Traffic Flow Stability," *IEEE Transactions on Vehicular Technology,* vol. 69, no. 7, pp. 6916-6927, 2020.

[21] J. Yang, G. Cao, W. Chen *et al.*, "Finite-Time Formation Control of Second-Order Linear Multi-Agent Systems With Relative State Constraints: A Barrier Function Sliding Mode Control Approach," *IEEE Transactions on Circuits and Systems II: Express Briefs,* vol. 69, no. 3, pp. 1253-1256, 2022.

[22] J. Zhao, X. Li, X. Yu *et al.*, "Finite-Time Cooperative Control for Bearing-Defined Leader-Following Formation of Multiple Double-Integrators," *IEEE Transactions on Cybernetics,* vol. 52, no. 12, pp. 13363-13372, 2022.

[23] Y. Liu, D. Yao, H. Li *et al.*, "Distributed Cooperative Compound Tracking Control for a Platoon of Vehicles With Adaptive NN," *IEEE Transactions on Cybernetics,* vol. 52, no. 7, pp. 7039-7048, 2022.

[24] D. Li, and G. Guo, "Prescribed Performance Concurrent Control of Connected Vehicles With Nonlinear Third-Order Dynamics," *IEEE Transactions on Vehicular Technology,* vol. 69, no. 12, pp. 14793-14802, 2020.